Microscopically Constrained Mean Field Models from Chiral Nuclear Thermodynamics

Ermal Rrapaj
Alessandro Roggero
Jeremy W. Holt

University of Washington & Institute for Nuclear Theory

July 28, 2016

Mean Field Models

A brief summary...

Current Models

- Skyrme $\longrightarrow$ more then 240 versions
- Relativsitic Mean Field $\longrightarrow$ more than 263 versions

Mean Field Models

A brief summary...

Current Models

- Skyrme $\longrightarrow$ more then 240 versions
- Relativsitic Mean Field $\longrightarrow$ more than 263 versions

Seems like a lot!

Pure neutron matter Equation of State (T = 0)

A brief history ...

Constraining mean field models

- Saturation density properties Dutra, Lourenco, Martins,Delfino PRC 85, 035201 (2012)
- Neutron matter uncertainty band from chiral effective theory Krüger,Tews,Hebeler,Schwenk PRC 88,025802 (2013)
- Low density neutron matter, ab-inito methods Brown, Schwenk PRC 91,049902 (2015)
- Compare many-body perturbation and Monte Carlo using χEFT Rrapaj, Roggero, Holt PRC 93, 065801 (2016)

New Constraints for neutron matter at T $= 0$

New Constraints for neutron matter at $T = 0$

Compare perturbative calculations with Quantum Monte Carlo

New Constraints for neutron matter at $T = 0$

Compare perturbative calculations with Quantum Monte Carlo

Quantum Monte Carlo in Configuration Interaction space

New Constraints for neutron matter at $T = 0$

Compare perturbative calculations with Quantum Monte Carlo

Quantum Monte Carlo in Configuration Interaction space

Potential Matrix Element

- NNLO_{opt} from Ekström et al
- $\text{N}^3\text{LO}, \lambda = 414$ MeV from Coraggio et al
- $\text{N}^3\text{LO}, \lambda = 450$ MeV from Coraggio et al
- $\text{N}^3\text{LO}, \lambda = 450$ MeV from Entem and Machleidt

New Constraints for neutron matter at T $= 0$

Compare perturbative calculations with Quantum Monte Carlo

Quantum Monte Carlo in Configuration Interaction space

Potential Matrix Element

- NNLO_{opt} from Ekström et al
- $\mathrm{N^3LO}, \lambda = 414$ MeV from Coraggio et al
- $\mathrm{N^3LO}, \lambda = 450$ MeV from Coraggio et al
- $\mathrm{N^3LO}, \lambda = 450$ MeV from Entem and Machleidt

Many-body perturbation to 3^{rd} order

Low density constraints for neutron rich matter

Relativistic Mean Field Models

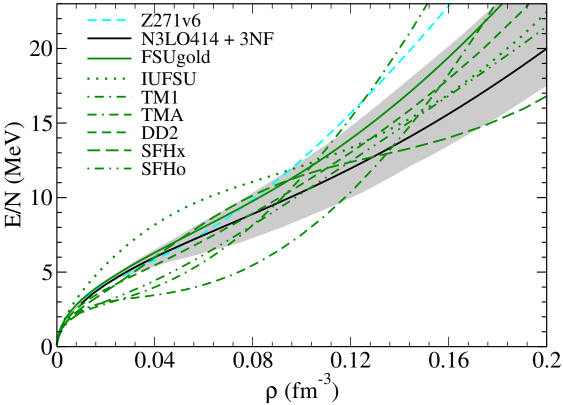

band from Krüger, Tews, Hebeler, Schwenk PRC 88, 025802 (2013)

Low density constraints for neutron rich matter

Relativistic Mean Field Models

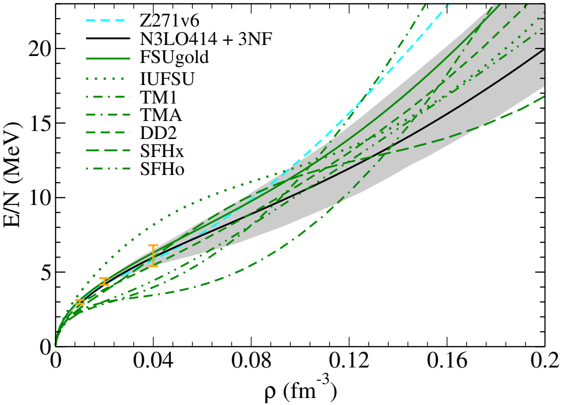

band from Krüger, Tews, Hebeler, Schwenk PRC 88, 025802 (2013)
(orange) constraints from Brown, Schwenk PRC 91, 049902 (2015)

Low density constraints for neutron rich matter

Relativistic Mean Field Models

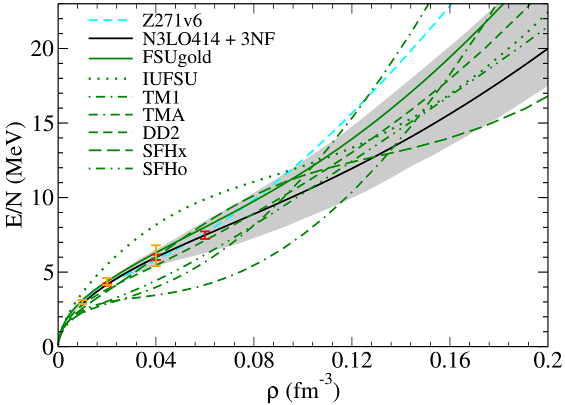

band from Krüger, Tews, Hebeler, Schwenk PRC 88, 025802 (2013)
(orange) constraints from Brown, Schwenk PRC 91, 049902 (2015)
(red) constraints from Rrapaj, Roggero, Holt PRC 93, 065801 (2016)

Low density constraints for neutron rich matter

Relativistic Mean Field Models

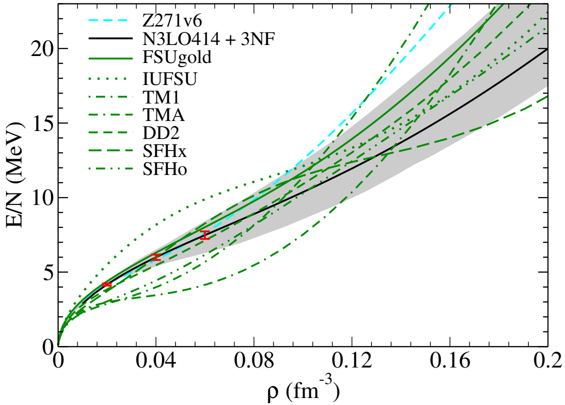

band from Krüger, Tews, Hebeler, Schwenk PRC 88, 025802 (2013)
(red) constraints from Rrapaj, Roggero, Holt PRC 93, 065801 (2016)

Low density constraints for neutron rich matter

(0.9, 1.0) Skyrme models from Brown, Schwenk PRC 91,049902 (2015)
UNEDEF: Lesinski et al, PRC 82, 024313 (2010), McDonell PRC 85, 024304 (2012), McDonell PRC 89, 054314 (2014)
(black) constraints from Rrapaj, Roggero, Holt PRC 93, 065801 (2016)

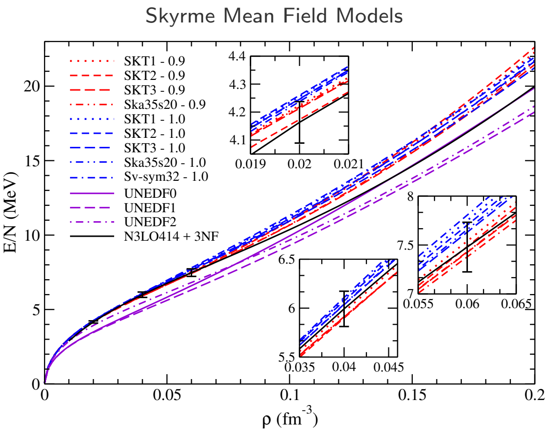

Low density constraints for neutron rich matter

(0.9, 1.0) Skyrme models from Brown, Schwenk PRC 91,049902 (2015)
UNEDEF: Lesinski et al, PRC 82, 024313 (2010), McDonell PRC 85, 024304 (2012), McDonell PRC 89, 054314 (2014)
(black) constraints from Rrapaj, Roggero, Holt PRC 93, 065801 (2016)

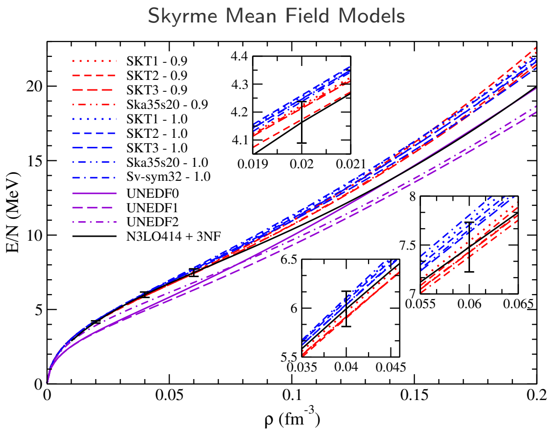

Found mean field models consistent with all constraints!

Low density constraints for neutron rich matter

(0.9, 1.0) Skyrme models from Brown, Schwenk PRC 91,049902 (2015)
UNEDEF: Lesinski et al, PRC 82, 024313 (2010), McDonell PRC 85, 024304 (2012), McDonell PRC 89, 054314 (2014)
(black) constraints from Rrapaj, Roggero, Holt PRC 93, 065801 (2016)

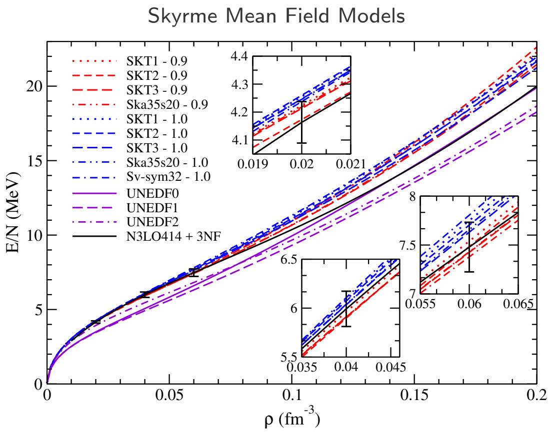

Found mean field models consistent with all constraints!

Not currently used in supernovae simulations!

Many-body perturbation theory at finite temperature

Wellenhofer, Holt, Kaiser, Weise PRC 89, 064009 (2014)

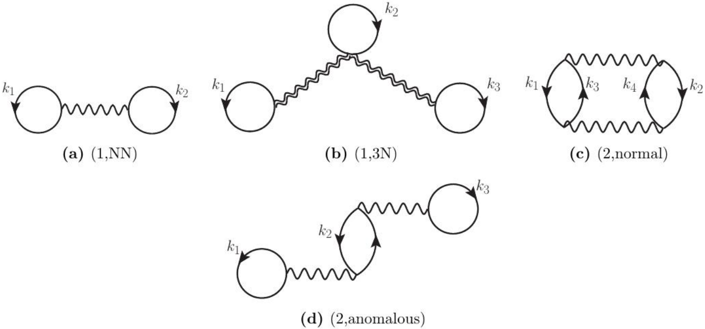

$T > 0$ EoS: Skyrme interactions and relativistic models

Rrapaj, Roggero, Holt PRC 93, 065801 (2016)

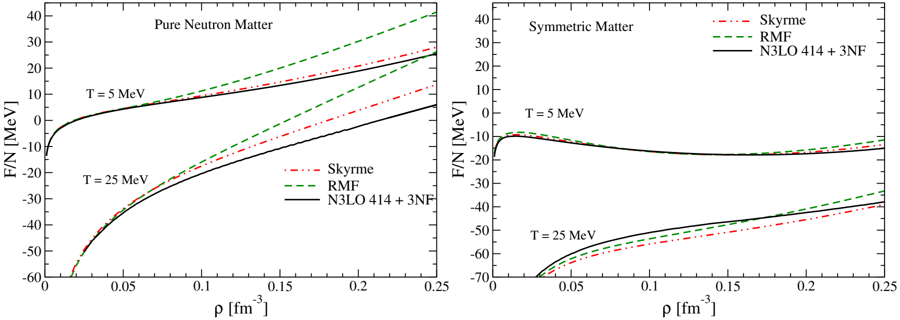

$T > 0$ EoS: Skyrme interactions and relativistic models

Rrapaj, Roggero, Holt PRC 93, 065801 (2016)

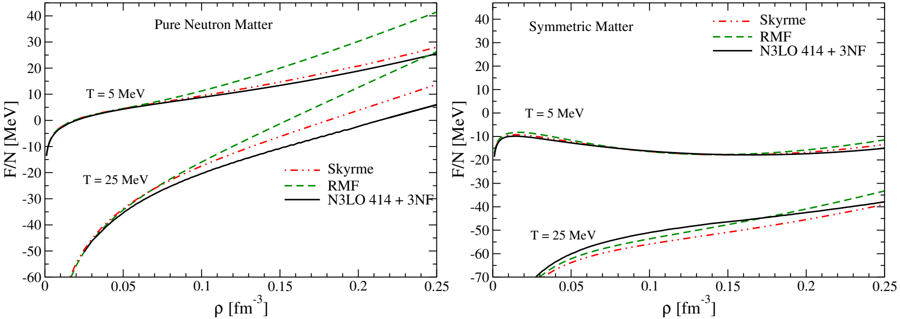

'Qualitatively' comparable with many-body calculations

Thermal Properties

Rrapaj, Roggero, Holt PRC 93, 065801 (2016)

$S = const$ trajectories

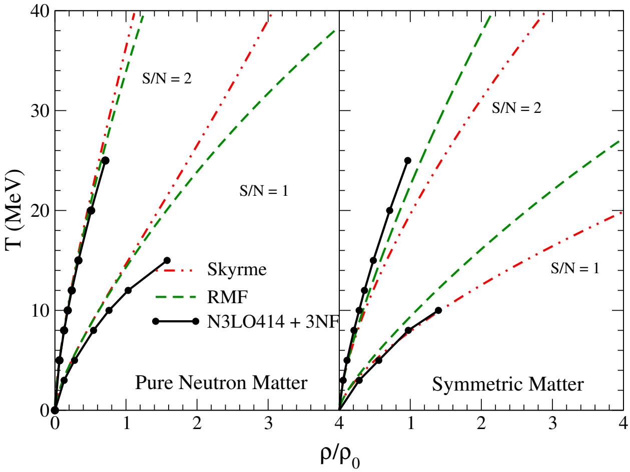

Core temperature uncertain!

Thermal Properties

Rrapaj, Roggero, Holt PRC 93, 065801 (2016)

$S = const$ trajectories

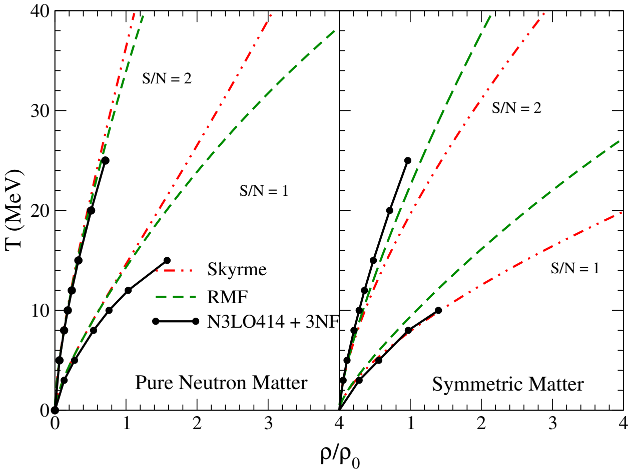

Beyond mean field signature !

ν spectra and nucleosynthesis

Nucleosynthesis

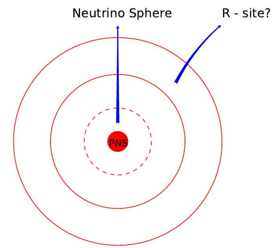

$\nu_e, \overline{\nu_e}$ decoupling region

- $T \approx 5 - 10$ MeV
- $n \lesssim 0.02$ fm^{-3}

R-process Conditions

- $S/N \geq 100 - 150$ at R-site
- Fast expansion time scale
- $Y_n \geq 0.6$

$\nu_e, \overline{\nu_e}$ impact on y_n

$$\nu_e + n \longleftrightarrow e^- + p$$

$$\overline{\nu}_e + p \longleftrightarrow n + e^+$$

Charged Current Reactions

ν_e absorption

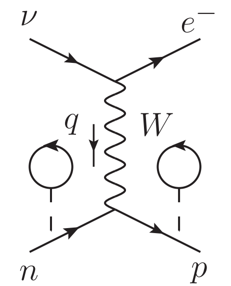

$$Q_{\text{value}} \equiv \omega = E_n(\vec{p}) - E_p(\vec{p} + \vec{q})$$

Charged Current Rate

$$\lambda^{-1} = \frac{2}{(2\pi)^5} \int d^3p_n \, d^3p_e \, d^3p_p \, \mathcal{W}_{fi}$$
$$\times \, \delta^{(4)}(p_{\nu_e} + p_n - p_e - p_p)$$
$$\times \, f_n(\xi_n)(1 - f_e(\xi_e))(1 - f_p(\xi_p))$$

where $\xi = E - \mu$, and

$$\mathcal{W}_{fi} = \frac{\langle |\mathcal{M}|^2 \rangle}{2^4 E_n E_p E_e E_{\nu_e}}$$
$$\langle |\mathcal{M}|^2 \rangle = \frac{1}{8} \, G_F^2 \, L^{\mu\nu} \Pi_{\mu\nu}$$

In medium dispersion relations

$$E_n(p) = \frac{p^2}{2M_n} + \Sigma_n^{Re}(p) + i\Sigma_n^{Im}(p)$$

Low Density: $E_n(p) \approx \frac{p^2}{2M_n^*} + U_n$

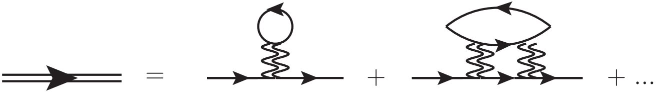

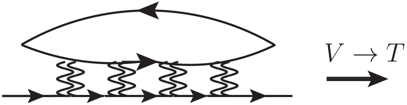

$$V_{Ps} = -\frac{\delta(q)}{q\ M}$$

Fummi(1955), Fukuda and Newton(1956)

Carged Current Opacities

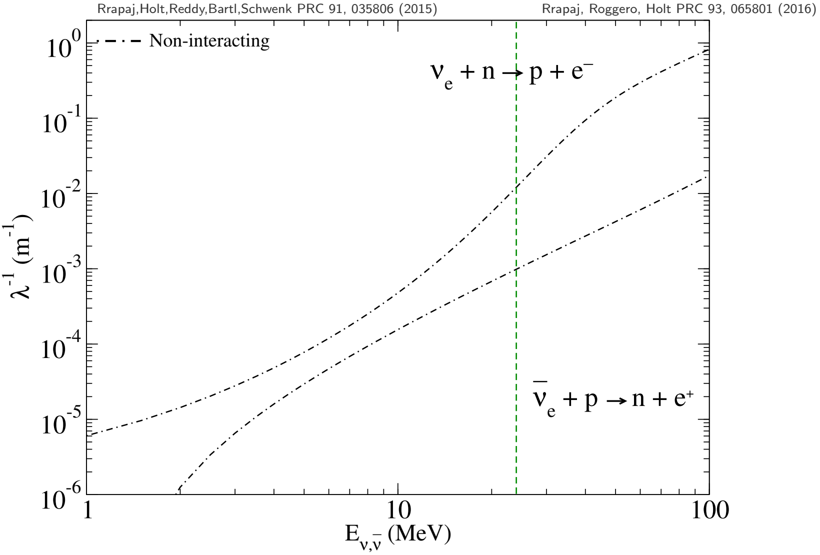

Carged Current Opacities

Rrapaj,Holt,Reddy,Bartl,Schwenk PRC 91, 035806 (2015)   Rrapaj, Roggero, Holt PRC 93, 065801 (2016)

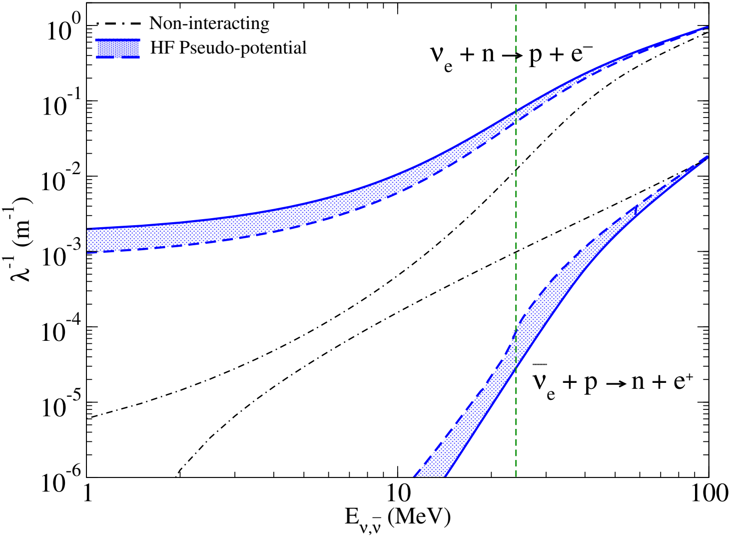

Carged Current Opacities

Rrapaj,Holt,Reddy,Bartl,Schwenk PRC 91, 035806 (2015)

Rrapaj, Roggero, Holt PRC 93, 065801 (2016)

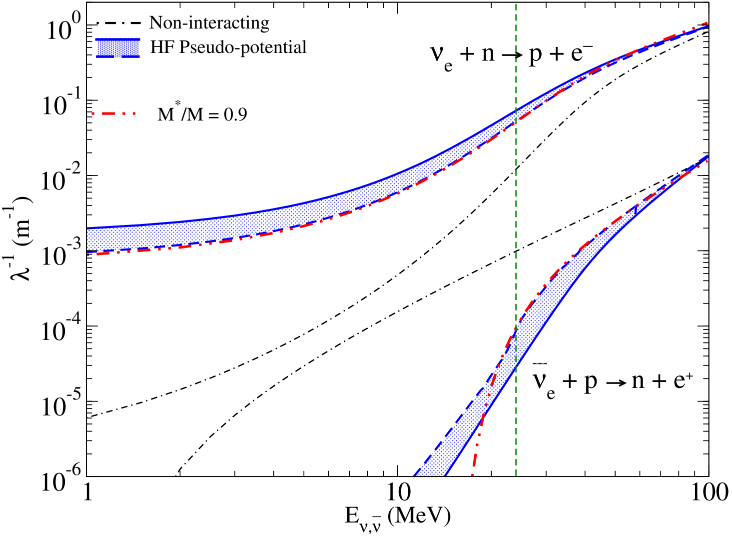

Carged Current Opacities

Rrapaj,Holt,Reddy,Bartl,Schwenk PRC 91, 035806 (2015)

Rrapaj, Roggero, Holt PRC 93, 065801 (2016)

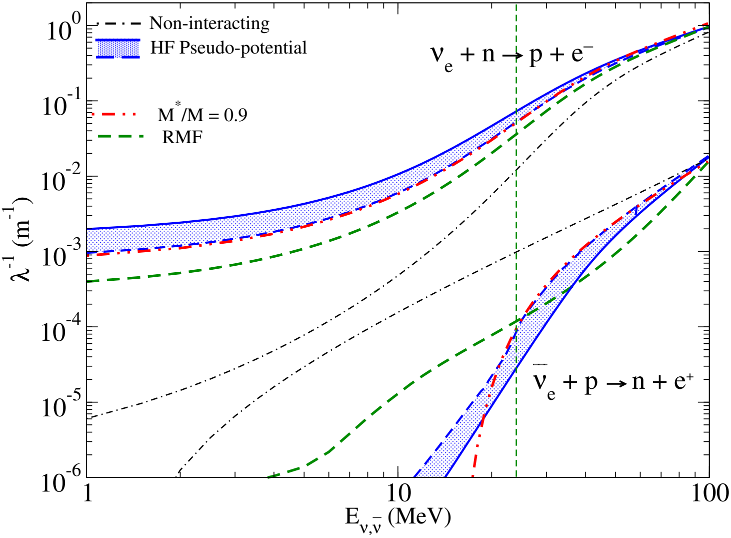

Carged Current Opacities

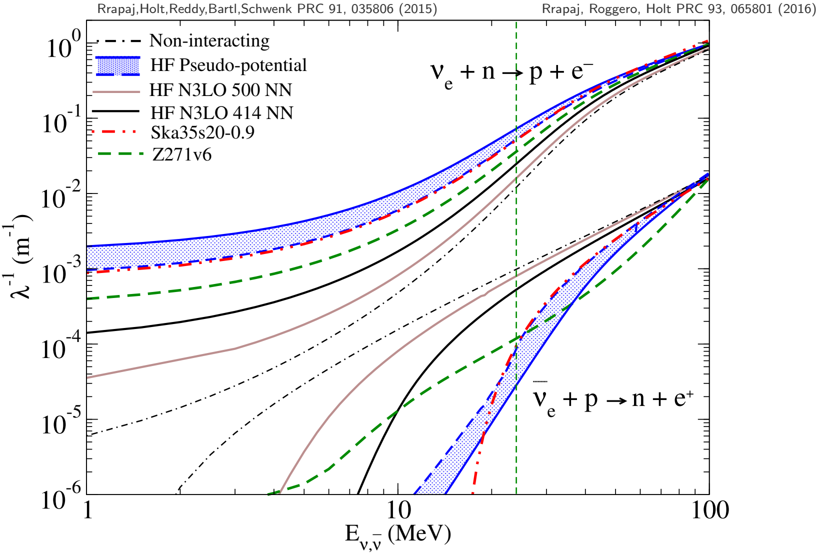

Mass Radius Relationship

(grey) band from Krüger, Tews, Hebeler, Schwenk PRC 88,025802 (2013)
(violet) constraint from Steiner, Lattimer, Brown Astrophys. J 765, L5 (2013)
Rrapaj, Roggero, Holt PRC 93, 065801 (2016)

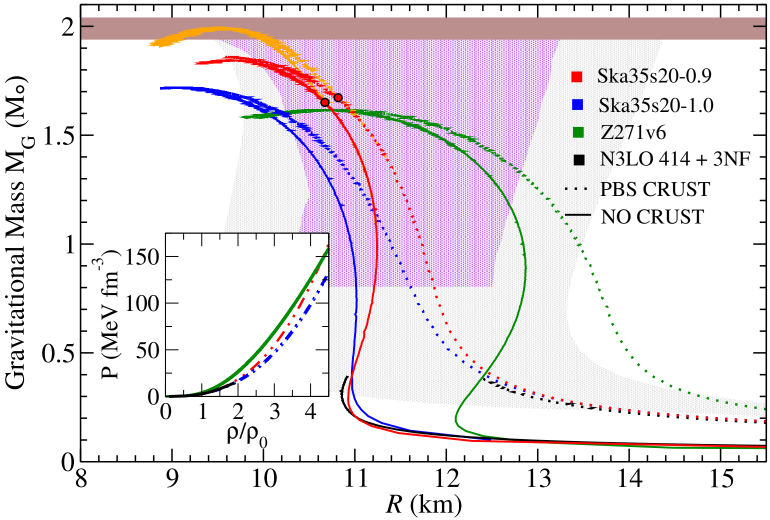

Thank You

- Sanjay Reddy
- Jeremy Holt
- Alessandro Roggero
- Alexander Bartl
- Achim Schwenk
- Luke Roberts

Finite Temperature: MF and MBPT

Rrapaj, Roggero, Holt. , arxiv:1510.00444 (2015)

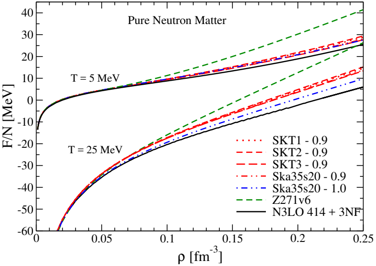

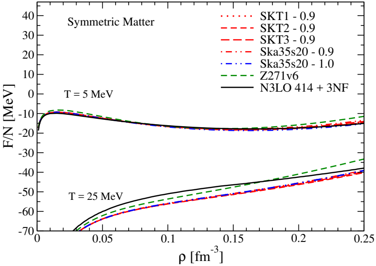

Dominant effect coming from $M^* \longrightarrow$ sp-properties !

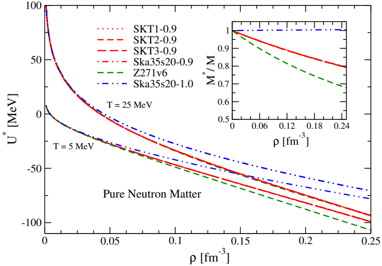

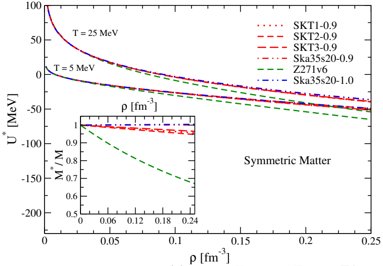

Pesudo Potential

Definitions

$$\text{Pseudo potential :} \quad \langle p | V^{pseudo}_{llSJ} | p \rangle = -\frac{\delta_{ISJ}(p)}{pM}$$

$$2^{nd} \text{ virial coefficient :} \quad b_2 = \frac{1}{\pi\sqrt{2}\,T} \int_0^\infty d\epsilon\, e^{-\epsilon/2T} \sum_{ISJ} (2J+1)\delta_{ISJ}(\epsilon) - 2^{-5/2} \tag{1}$$

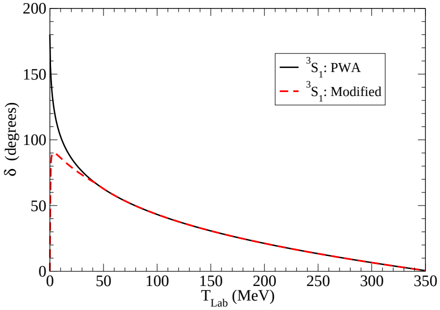

Comparison with virial calculations

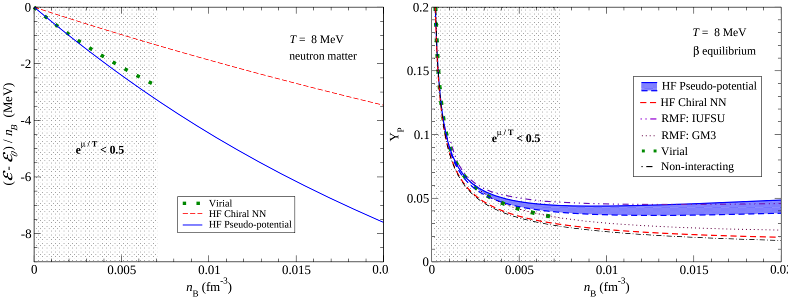

Convergence of MBPT: Neutron matter at T = 0

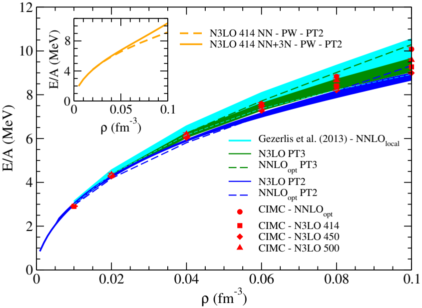

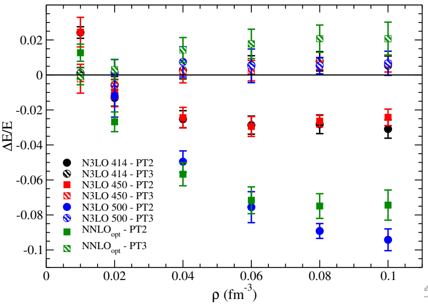

CIMC: Short Introduction I

CIMC: Projection Method in Fock Space

$$|\Psi_0\rangle = \lim_{N_\tau \to \infty} \mathcal{P}^{N_\tau} |\Psi_{\mathrm{I}}\rangle. \qquad (2)$$

$$\mathcal{P} = e^{-\Delta\tau(H - E_T)}$$

Sign Problem

If we introduce the sign function

$$\mathfrak{s}(\mathbf{m},\mathbf{n}) = sign\left(\frac{\langle \Phi_G|\mathbf{m}\rangle}{\langle \mathbf{n}|\Phi_G\rangle}\langle \mathbf{m}|H|\mathbf{n}\rangle\right), \qquad (3)$$

$$\langle \mathbf{m}|\mathcal{H}_\gamma|\mathbf{n}\rangle = \begin{cases} -\gamma\frac{\langle \Phi_G|\mathbf{m}\rangle}{\langle \mathbf{n}|\Phi_G\rangle}\langle \mathbf{m}|H|\mathbf{n}\rangle & \mathfrak{s}(\mathbf{m},\mathbf{n}) > 0 \\ \frac{\langle \Phi_G|\mathbf{m}\rangle}{\langle \mathbf{n}|\Phi_G\rangle}\langle \mathbf{m}|H|\mathbf{n}\rangle & \text{otherwise} \end{cases}, \qquad (4)$$

while the diagonal elements are:

$$\langle \mathbf{n}|\mathcal{H}_\gamma|\mathbf{n}\rangle = \langle \mathbf{n}|H|\mathbf{n}\rangle + (1+\gamma)\sum_{\substack{\mathbf{n}\neq\mathbf{m} \\ \mathfrak{s}(\mathbf{m},\mathbf{n})>0}} \frac{\langle \Phi_G|\mathbf{m}\rangle}{\langle \mathbf{n}|\Phi_G\rangle}\langle \mathbf{m}|H|\mathbf{n}\rangle \qquad (5)$$

CIMC: Short Introduction II

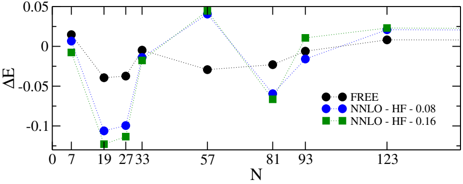

Figure : Finite-size errors in the energy per particle as a function of the number of particles per spin-isospin species. The results shown are for a free gas as well as for Hartree-Fock calculations with the NNLO$_{opt}$ interaction at the two densities $\rho = \rho_0$ and $0.5\rho_0$.

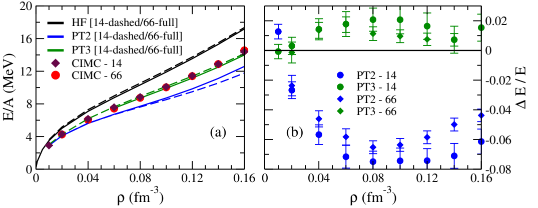

Figure : (panel (a)): energy per particle in PNM computed with $N = 14$ and 66 neutrons from CIMC and MBPT using the NNLO$_{opt}$ chiral two-nucleon potential. (panel (b)): relative differences between the results from CIMC and MBPT at second and third order using $N = 14$ and 66.

Constraints on infinite matter porperties

Name	compatible	K_m [MeV]	K' [MeV]	J [MeV]	L [MeV]	$K_{\tau,v}$ [MeV]	$S(\rho/2)/J$	$3P_{PNM}/L\rho_0$
Ska25s20 - 0.9	-	220	413	32.1	50.9	-345	0.66	1.00
Ska35s20 - 0.9	+	240	378	32.2	53.6	-374	0.65	0.98
SKT1 - 0.9	+	238	382	32.6	55.3	-378	0.65	1.00
SKT2 - 0.9	+	240	385	33.1	58.0	-385	0.64	1.00
SKT3 - 0.9	+	237	382	32.0	52.6	-370	0.65	0.99
Sv-sym32 - 0.9	-	234	384	31.5	49.5	-360	0.66	1.01
Ska25s20 - 1.0	-	220	415	32.0	46.4	-355	0.67	1.04
Ska35s20 - 1.0	+	240	379	32.2	50.6	-385	0.66	1.02
SKT1 - 1.0	+	237	384	32.5	51.5	-386	0.66	1.02
SKT2 - 1.0	+	236	387	32.3	50.4	-381	0.66	1.02
SKT3 - 1.0	+	237	385	33.0	48.9	-377	0.66	1.02
Sv-sym32 - 1.0	+	237	375	32.0	47.7	-387	0.66	1.06
FSUgold	-	230	524	32.6	60.4	-276	0.60	1.00
Z271v5	+	270	734	34.0	73.9	-389	0.57	1.0
Z271v6	+	270	734	33.8	70.9	-388	0.57	1.0
N3LO414 + 3NF	+	223	270	32.5	53.8	-424	0.70	1.05
Range of constraint		190-270	200-1200	30-35	40-76	-760 to -372	0.57-0.86	0.90-1.10

$$
\begin{aligned}
K_m =& 9\left.\frac{\partial P}{\partial \rho}\right|_{\rho_0}, \quad P = \rho^2\frac{\partial(E/N)}{\partial\rho}, \quad K' = -27\rho_0^3\left.\frac{\partial^3(E/N)}{\partial\rho^3}\right|_{\rho_0}, \\
J =& S(\rho_0) = \left.\frac{\partial(E/N)}{\partial\delta_{np}^2}\right|_{\rho_0}, \delta_{np} = \frac{\rho_n-\rho_p}{\rho_n+\rho_p}, \quad L = 3\rho_0\left.\frac{\partial S}{\partial\rho}\right|_{\rho_0} \\
K_{\tau,v} =& K_{\mathrm{sym}} - L\left(6+\frac{K'}{K_m}\right), \quad K_{\mathrm{sym}} = 9\rho_0^2\left.\frac{\partial^2 S}{\partial\rho^2}\right|_{\rho_0}
\end{aligned} \qquad (6)
$$